NUMERICAL INVESTIGATION ON THE HEAT TRANSFER OF AIR/HELIUM PRECOOLER FOR AIR-BREATHING PRE-COOLED ENGINE

by

Xin WEI, Feng JIN, Zhaohui YAO, and Honghu JI*

College of Energy and Power Engineering, Nanjing University of Aeronautics and Astronautics, Nanjing, China

Installing a precooler behind the intake is an effective approach for hypersonic air-breathing pre-cooled engine to cool the hot incoming air. Synergetic air-breathing rocket engine is a revolutionary hypersonic air-breathing pre-cooled engine with complex thermodynamic cycle i.e. air cycle, helium cycle. Air/helium precooler is a key component and its configuration and operating condition have great effect on the performance characteristics of air-breathing pre-cooled engine. Thus, the minimum periodic flow and heat transfer model of the precooler are established. The effects of key parameters on the heat transfer performance of precooler are numerically studied. The results indicate that: when the tube row number increases from 7 to 15, the average heat transfer coefficient of air side decreases by 57%, the heat exchange rate increases by 19%, and effectiveness increases by 18.4%. The tube transverse pitch can enhance the heat transfer coefficient of air and helium side, while the heat exchange rate decreases by 33 % when the tube transverse pitch increases from 1.5 to 3.5. The helium inlet velocity can improve the heat transfer performance of precooler and reduce the flow resistance of air side.

Key words*: precooler, heat transfer coefficient, helium coolant, numerical simulation, air-breathing pre-cooled engine*

Introduction

Power is the most critical and decisive technology for hypersonic vehicles. Turbine, rocket and scramjet combined engines are the hot spots in the research of hypersonic vehicle propulsion technology [1]. Hypersonic vehicles put forward higher requirements for new propulsion systems, such as wide speed range, reusability, single-stage orbit entry, high specific impulse and thrust-weight ratio [2-4]. In order to prevent the inlet stagnation temperature from exceeding the heat resistance limit of the compressor and maintain the performance of the power system, the precooler must be used to reduce the inlet temperature and increase the compressor pressure ratio in the intake system when the air-breathing combined engine flies at high Mach number. This is of great significance for the hypersonic vehicle to expand the flight envelope and improve the thrust-to-weight ratio of the engine [5, 6]. Precooler is a key technology

with great application potential and development space. Applying the powerful cooling capacity of hydrogen fuel can further improve the efficiency of aero-engine, which is also one of the key technologies for complete decarbonization of aero-engine.

Figure 1. Structure of SABRE precooler

At present, there is an urgent need to develop a compact precooler with micro-channel for air-breathing combined engine [7, 8]. The SABRE engine [9] in the UK and the ATREX engine [10] in Japan have adopted the compact precooler structure with micro-channel, and the most noteworthy precooler scheme is the SABRE precooler scheme [11-14]. The SABRE engine adds a helium Brayton cycle between hydrogen and air, and the high efficiency heat transfer between hot air and low temperature helium is realized by precooler [15, 16]. As shown in fig. 1, SABRE precooler is composed of a series of spiral micro-channel modules. Air-flows through the tiny clearance between the tubes, and the low temperature helium exchanges heat with the external hot air in the micro-channel [17]. The micro-channel used in SABRE precooler have total length of more than 1000 kilometer, the tube diameter of 1 mm, the tube thickness of 20 μm, and the total heat transfer rate of more than 400 MW [18].

In view of the huge application potential of the precooler in the air-breathing pre-cooled engine, many researchers have made consistent efforts in exploring the flow and heat transfer of precooler, mainly focusing on numerical simulation, experimental research and simplified calculation methods. Li *et al*. [19] numerically investigate the effects of geometry size and compactness of tube arrangement on the flow and heat transfer characteristics of the precooler. Pan *et al*. [20] and Li *et al*. [21] investigated the thermal performance of staggered mini-tube bundle as the compact precooler, the inlet pressure, inlet temperature, transverse pitch, coolant velocity. Murray *et al*. [22] built a small pre-cooling heat exchanger called JMHX with 0.38 mm tubes and tested the performance of heat exchange with helium and nitrogen as coolant, it revealed that the Kays and London Stanton and friction factor correlations remained applicable. Li *et al*. [23] proposed a segmental method to evaluate the performance of micro-channel heat exchanger for precooled engines and performed experimental study to validate the method. Webber *et al*. [16] experimentally studied the convective heat transfer capacity of staggered tube bundles similar to SABRE precooler in low speed wind tunnel. Moreover [24-28] have established simplified heat transfer models of the precooler in the 1-D thermodynamic cycle analysis of air-breathing pre-cooled engine, but the 1-D heat transfer model is too simple to reflect the real structure change of the precooler on the performance of the precooler.

Although lots of research about the precooler for hypersonic air-breathing pre-cooled engine has been carried out, there are still some deficiencies in the precooler that deserve further study. At present, the flow and heat transfer characteristics of helium in the precooler at supercritical state have not been considered in the research. Furthermore, most of the research objects are traditional staggered straight tube bundles, which are quite different from the structure of precooler in fig. 1. Therefore, considering the actual boundary conditions of the precooler during hypersonic flight and the supercritical state of helium, it is definitely worth exploring the influence of the structural parameters and boundary parameters on the performance of the precooler for hypersonic vehicles. To this end, the minimum periodic flow and heat transfer model
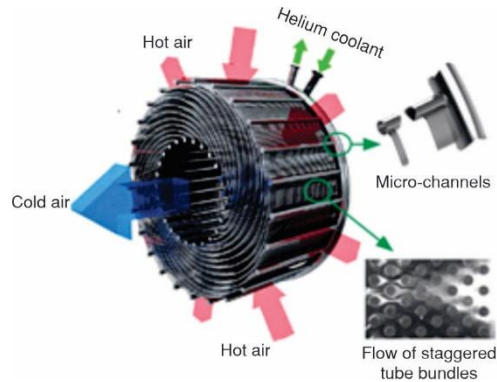
Wei, X., *et al.*: Numerical Investigation on the Heat Transfer of …
THERMAL SCIENCE: Year 2024, Vol. 28, No. 2A, pp. 913-927

915

of the precooler are established. The effects of key parameters such as tube transverse pitch, tube row number, and helium inlet velocity on the heat transfer characteristics of the air/helium precooler are discussed, and this can provide reliable theoretical basis for the practical engineering design of the precooler.

The air/helium precooler model for hypersonic air-breathing pre-cooled engine

As shown in fig. 2, the air/helium precooler is installed behind the intake. The high-speed air-flow is decelerated and heated by the shock wave. As the flow area increases when the hot air-flow into the precooler, the velocity of air-flow is further reduced. The schematic

Figure 2. Schematic of the intake and precooler

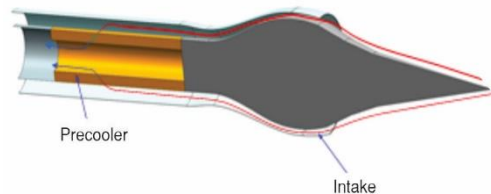diagram of the air/helium precooler model is shown in fig. 3. The precooler is composed of main pipes, branch pipes and precooler slices. The precooler slice consists of four rows of micro-channels arranged in an equilateral triangle shape, and rotates around the center of the circle to form a radial arrangement. There are 18 precooler slices in total, and the axial section of precooler slice is shown in fig. 4. The outer diameter of the micro-channel is 1 mm, the wall thickness is 0.05 mm, and the material is inconel 718. Low temperature and high pressure helium flows from the inner main pipe of precooler into each branch pipe, then into each micro-channel to gradually absorb the heat of hot air. Subsequently, helium is collected into the outer branch pipe and eventually flows into the outer main pipe. Meanwhile, the hot air-flows through the micro-channels and is gradually cooled by helium.
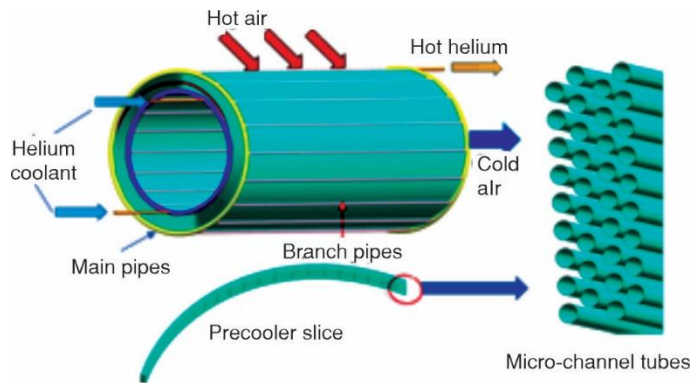

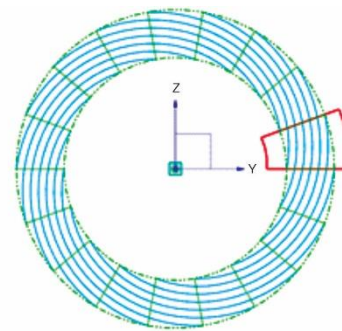**Figure 3. Structure of air/helium precooler**

Figure 4. The axial section of precooler slice

Numerical methods

Computational model and mesh dividing methods

It can be seen from fig. 4 that the precooler is characterized by periodic repetition in the circumferential direction, and so do the flow and heat transfer of helium and air. The red sector in fig. 4 is the smallest periodic unit, which can be taken for numerical simulation model. The computational model is shown in fig. 5. Each precooler slice is composed of four rows of

micro-channels, and tube row number rn is the number of precooler slices in the computational model. As shown in fig. 6, the array of micro-channels is arranged into equilateral triangle. Since the flow and heat transfer of helium have the characteristics of periodic repetition, the helium state parameters are the same at 1 and 1', 2 and 2', 3 and 3',…, 8 and 8' for the precooler, which could be set as the periodic boundary conditions. Since the included angle of the sector is relatively small, the air-flowing at the upper and lower boundaries of the sector can be approximately regarded as the same, which can be set as periodic boundary conditions.
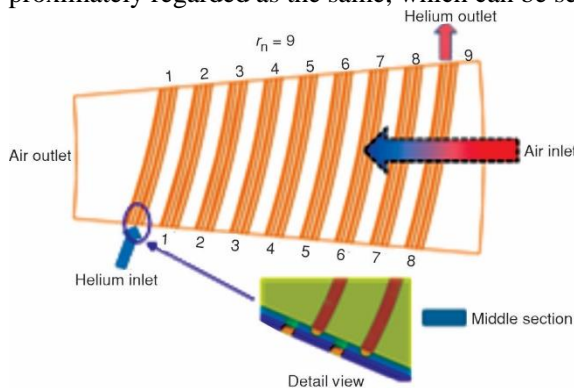

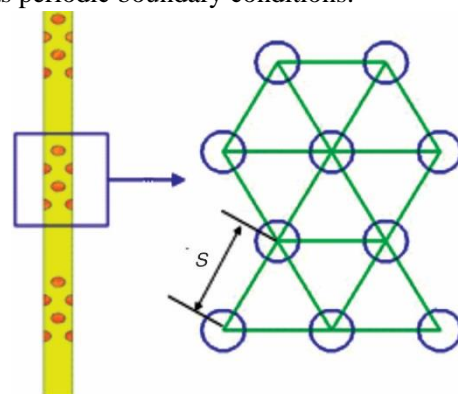**Figure 5. Computational model for the precooler**

Figure 6. Cross arrangement of the tube array for precooler slice

The unstructured meshes are firstly generated to spatially discretize the computational domain by ICEM 20.0. Very fine mesh is adopted in the near-wall region to capture the boundary-layer and flow separation. The height of the first layer of mesh near the wall on the air side is 0.0028 mm, the growth ratio is 1.2, and the number of boundary-layers is 10. For the helium side, the height of the first layer of mesh is 0.0011 mm, the growth ratio is 1.2, and the number of boundary-layers is 10. The representative mesh is exhibited in fig. 7. Enhanced wall treatment is adopted, the dimensionless $y+$ set to be smaller than 5. The validation of mesh independence is shown in fig. 8. It can be seen that when the grid number is greater than 11.9 million, the air outlet temperature changes slightly. Compared to the mesh with finest mesh (16.24 million), the mesh with 11.9 million elements shows a discrepancy of 0.72% on air outlet temperature, which has relatively higher accuracy and less computational consumption. Therefore, the mesh division method with 11.9 million elements is selected as the mesh division strategy for each model.
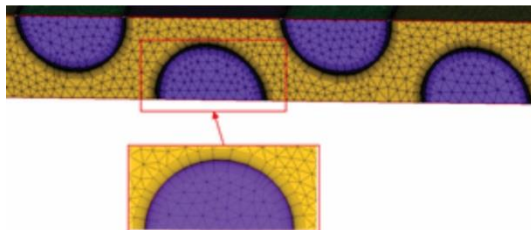

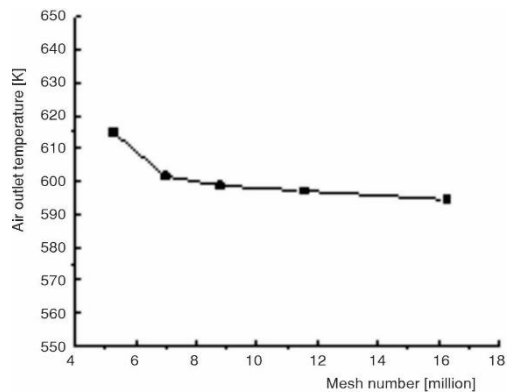**Figure 7. The detail mesh of the computational domain**

Figure 8. Validation of mesh independence

Boundary conditions and numerical methods

As shown in fig. 5, the pressure inlet boundary condition is adopted for the air inlet, the total temperature and pressure are given according to actual operational environment of the precooler. The pressure outlet boundary condition is applied at the air outlet and helium outlet, and the target flow rate of air outlet is given according to actual operational environment of the precooler. The static pressure of helium outlet is 20 MPa. The helium inlet is set as the velocity inlet boundary condition, and the inlet static temperature is 340 K. Except for the helium inlet and helium outlet, the walls on both sides of the circumference are set as periodic boundary conditions. Besides, symmetric boundary condition is applied at the symmetry plane, and the tube wall is set as coupled heat-transfer. Since the helium cycle in the SABRE engine is a closed cycle, the total helium flow rate is set to a constant value [29]. Moreover, the flow rate of air side remains unchanged at the design point [30]. Therefore, the total air-flow rate and helium flow rate of the precooler as well as the total axial length of the precooler are constant values, but the air-flow rate and helium flow rate of the computational model increase with the increase of the tube transverse pitch. The boundary conditions and the detail setting for tube transverse pitch, tube row number, and helium inlet velocity on the heat transfer characteristics of the air/helium precooler are shown in tabs. 1 and 2.

Table 1. Boundary conditions and the detail setting for
the effect of tube row number and tube transverse pitch

Boundary conditions	Helium flow rate [kgs^{-1}]	Helium inlet temperature [K]	Air inlet total pressure [Pa]	Air inlet total temperature [K]	Air-flow rate [kgs^{-1}]
Value	44	340	225680	695.7	230

Table 2. Boundary conditions and the detail setting for
the effect of helium inlet velocity

Boundary conditions	Helium inlet temperature [K]	Air inlet total pressure [Pa]	Air inlet total temperature [K]	Air-flow rate [kgs^{-1}]
Value	340	225680	695.7	230

The physical properties of air and supercritical helium are determined by the NIST software. The air density is defined as the density of ideal gas. The specific heat capacity and thermal conductivity are functions of temperature and a polynomial function is used for the fitting. The kinematic viscosity is given by the Sutherland formula. Supercritical helium is a single-phase state and will not present a two-phase state due to the increase in temperature. The supercritical helium in the precooler is far from the critical point (5.19 K, 0.228 MPa) and its physical parameters do not change as drastically as those near the critical point. Therefore, in this present paper, the supercritical helium in the precooler tube belongs to single-phase heat transfer. The pressure of the precooler is basically constant due to the small flow resistance of supercritical helium, while the temperature varies greatly. Therefore, the kinematic viscosity, specific heat capacity, and thermal conductivity are also almost exclusively temperature de-pendent and the relationships between physical properties of helium and temperature are shown in fig. 9.

The CFD solver used in the present study is FLUENT 20.0, flux difference scheme adopts ROE-FDS, Second-order upwind scheme is used to solve for discretization schemes of pressure, density, momentum and energy. The enhanced wall function is used to solve the flow and heat transfer in the viscous sublayer to improve the simulation accuracy of flow and heat transfer in the near wall region.
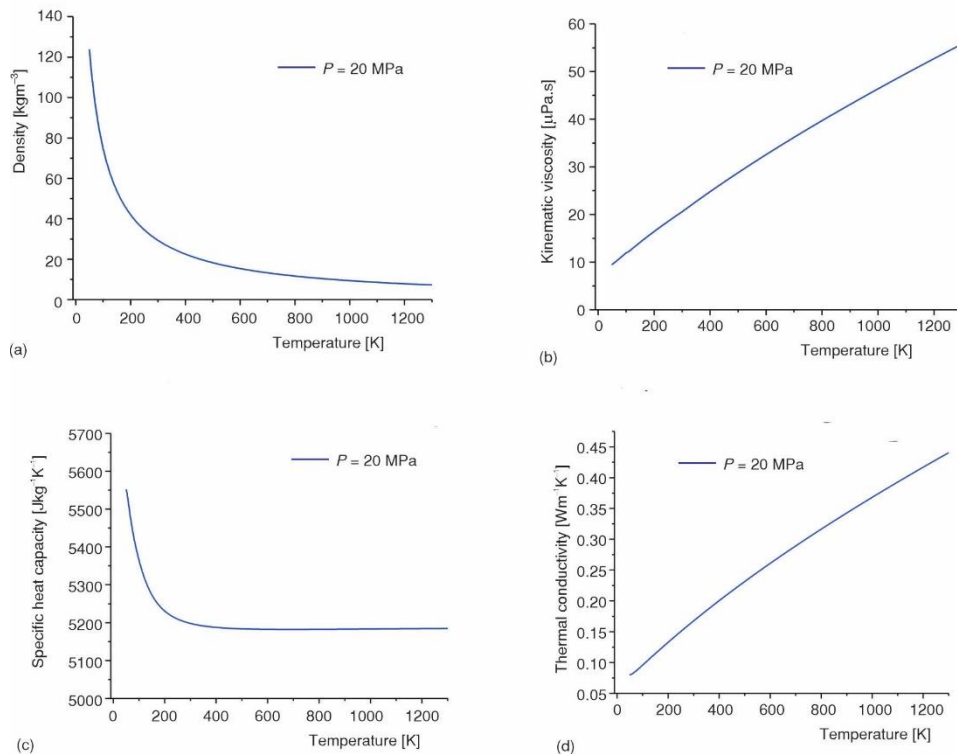
Figure 9. The relationships between physical properties of helium and temperature;
(a) density, (b) kinematic viscosity, (c) specific heat capacity, and (d) thermal conductivity

Table 3 shows the values of key parameters for the numerical simulation of the precooler. By controlling a single variable, studies have been conducted for tube transverse pitch, tube row number, and helium inlet velocity on the heat transfer characteristics of the air/helium precooler.

Table 3. The values of key parameters for the numerical simulation of the precooler

Parameter	Value
Tube row number	7, 9, 11, 13, 15
Tube transverse pitch [*S/D*]	1.5, 1.7, 2, 2.5, 3.5
Helium inlet velocity [ms^{-1}]	5.57, 6.58, 7.59, 8.61

Heat transfer validation

An experimental study of the compact precooler module JMHX was carried out in [26], and the accuracy of the numerical calculation method was verified by comparison with the numerical simulation results. The JMHX is a 40 mm × 38.95 mm × 3.762 mm structure with 415 tubes of 0.38 mm in diameter, arranged in 10 rows and 83 columns, as shown in fig.10. The coolant in the tube is cryogenic high pressure helium or nitrogen. Experiments in the literature with an internal coolant of helium and a heat capacity ratio of 1 were selected for comparative analysis. Figure 11 has shown the comparison between the numerical and experimental results of the helium outlet temperature of each tube for different turbulence models. It can be found that the numerical results of the first few rows of tubes near the air inlet have a relatively

large error with the experimental results, and the numerical results of the temperature for the last few rows of tubes have a small error with the experimental results. This may be caused by the large temperature difference between the inside and outside fluid of the first few tube rows, resulting in large deformation of the first few tube rows. Taken together, SST-$k\omega$ turbulence model was closer to the experimental results than other turbulence models, and the SST-$k\omega$ turbulence model was thus chosen for turbulence model of numerical simulation in this present paper.
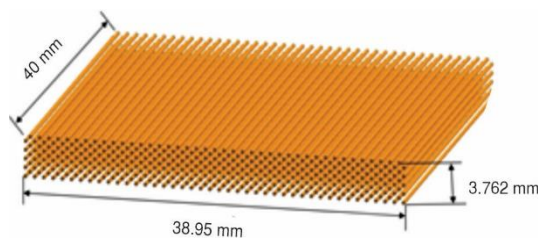

Figure 10. Geometric model of JMHX

Figure 11. The relationship of helium outlet temperature with the tube row number along the flow direction based on different turbulence models

Parameters definition of flow and heat transfer characteristic

When the fluid inside the tube is turbulent, the average surface heat transfer coefficient remains basically the same as long as the length-to-diameter ratio is greater than 60 [31]. Therefore, the average surface heat transfer coefficient inside the tube is approximately equal to the local heat transfer coefficient of the fully developed section. The local surface heat transfer coefficient inside the tube is defined as:

$$h_i = \frac{q}{t_w - t_f} \tag{1}$$

where t_w is the average inner wall temperature of the tube, q – the local heat flux, and t_f – the average fluid temperature of the local section.

The heat exchange rate, Q, is usually used to evaluate the heat transfer performance of the precooler. When the heat transfer of heat exchanger reaches a steady-state, the following energy conservation formula is as:

$$Q = \dot{m}_{air, pre} c_{p,air} \Delta T_{air} = \dot{m}_{He,pre} c_{p,He} \Delta T_{He} \tag{2}$$

where ΔT_{He}, ΔT_{air} denote the temperature difference between the inlet and outlet of helium and air, respectively.

For the SABRE engine precooler, it is difficult to directly calculate the heat transfer coefficient of the air side surface due to the complexity of the structure. In this present paper, the average heat transfer coefficient of the air side is obtained by indirect method to evaluate the heat transfer intensity of the air side. The following describes the solution method of the average heat transfer coefficient of the air side.
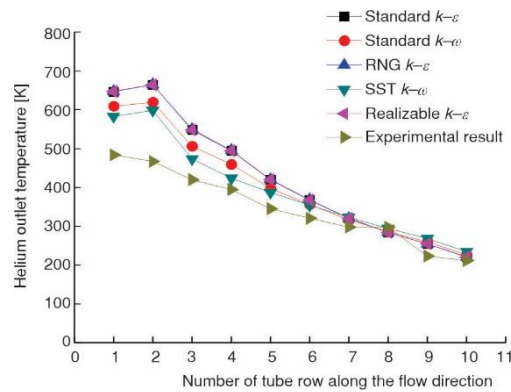
The total heat transfer coefficient, K, of the precooler is defined as:

$$K = \frac{Q}{A\psi \left(\Delta T_m\right)_{\text{ctf}}} \tag{3}$$

where A is the shell-side area of the precooler, $(\Delta T_m)_{\text{ctf}}$ – the logarithmic mean temperature difference of counterflow heat exchanger, ψ – the correction factor, which could be calculated according to [29]. According to the tube arrangement of the precooler, the range of ψ is calculated to be 0.98~1, indicating that the fluid-flow form of the precooler is close to the counterflow arrangement. The total heat transfer coefficient, K, of the precooler can be also expressed by the concept of thermal resistance:

$$K = \frac{1}{\dfrac{1}{h_{\text{He}}} + R_{\text{w}} + R_{\text{S}} + \dfrac{1}{h_{\text{Air}}}\dfrac{d_{\text{O}}}{d_{\text{i}}}} \tag{4}$$

where d_{o} and d_{i} are the outer and inner diameter of the tube, respectively. Due to the thin wall thickness of the capillary tube, the thermal conduction resistance, R_{w}, and fouling resistance, R_{S}, are neglected, and the average heat transfer coefficient on the air side can be calculated as:

$$h_{\text{Air}} = \left[\left(\frac{1}{K} - \frac{1}{h_{\text{He}}}\right)\frac{d_{\text{i}}}{d_{\text{o}}}\right]^{-1} \tag{5}$$

The effectiveness of the heat exchanger is defined as $\varepsilon = \left(t' - t''\right)_{\max} / \left(t_1' - t_2'\right)$ [32]. The denominator is the maximum temperature difference that can occur in the heat exchanger for the fluid, and the numerator is the larger of the actual temperature difference for the cold fluid or the hot fluid in the heat exchanger.

Analysis and discussion

Effect of tube row number on the heat transfer performance of air/helium precooler

The number of tube rows is the number of precooler slices that the air-flows along the radial direction, as shown in fig. 5. The number of tube rows determines the heat exchange area and compactness of the precooler, as is shown in tab. 4, thus affecting the heat exchange performance of the precooler. The influence of tube row number on the heat transfer of the precooler was studied under the condition that the boundary conditions, the tube spacing, the total axial length of the precooler, and the inner and outer diameters are constant.

Table 4. Relationship between tube row number and compactness of precooler

Tube row number	7	9	11	13	15
Compactness of precooler [m²/m³]	303.34	383.82	461.04	541.90	624.10

To have a better understanding of the effect of tube row number on the heat transfer of air/helium precooler, the relationship between heat transfer coefficient of air side and helium side with tube row number is shown in fig. 12. It can be seen that the heat transfer coefficient of air side and helium side are decreasing with the increment of tube row number. The increment of tube row number can cause pretty decrease of the heat transfer coefficient of air side, it decreases by amount 57% at $r_n = 15$ compared the value at $r_n = 7$. However, the decrease of the heat transfer coefficient of helium side is not pronounced, and it decreases only by amount 3.8% at $r_n = 15$ compared the value at $r_n = 7$. This phenomenon is probably due to the fact that

Wei, X., *et al.*: Numerical Investigation on the Heat Transfer of …
THERMAL SCIENCE: Year 2024, Vol. 28, No. 2A, pp. 913-927

921

the number of tube rows has no effect on the helium inlet velocity, while an increment in the number of tube rows means an increment in the length of the precooler slices and thus the heat transfer enhancement on the inlet of helium side has attenuation on the average helium heat transfer coefficient. For the air side, an increment in the number of tube rows results in a linear increment in the heat transfer area. However, the increment in logarithmic mean temperature difference and heat exchange rate, Q, is not as significant as the increment in heat transfer area. According to eqs. (1) and (3), the increment of tube row number can cause pretty decrease of the heat transfer coefficient of air side.
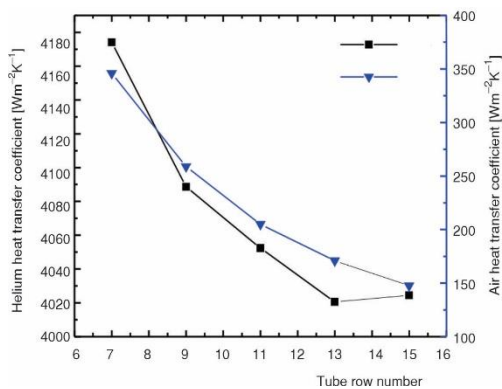

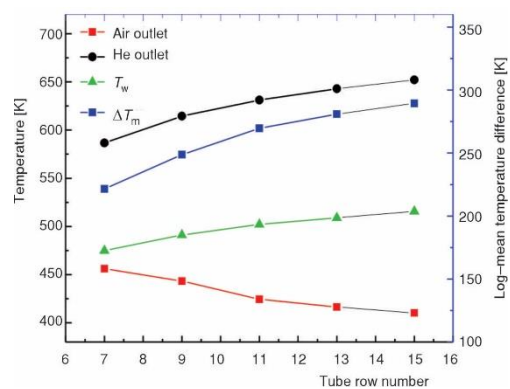**Figure 12. Effect of tube row number on heat transfer coefficient of air side and helium side**

Figure 13. Effect of tube row number on temperature of air, helium outlet, tube wall, and ΔT_m

Figures 13 and 14 show that effect of tube row number on the temperature of air, helium outlet, logarithmic mean temperature, ΔT_m, effectiveness and heat exchange rate of precooler. It can be seen that an increment of tube row number leads to a decrement in the air outlet temperature, an increment in the heat exchange rate, an increment in the heat transfer effectiveness, and a corresponding increment in the average tube wall temperature. Although the increment in the number of tube rows reduced the heat transfer coefficient, the overall precooling capacity of the precooler is enhanced due to the increase of heat transfer area. Nevertheless, it can also be seen from fig. 13 that when tube row number is greater than 11, the growth rate of heat exchange rate is also decreasing. From 7 rows to 11 rows, the heat transfer power increases by 13% and effectiveness increases by 12.5%, while from 11 rows to 15 rows, the heat transfer
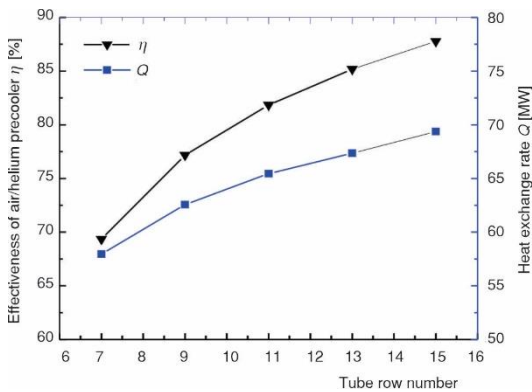

Figure 14. Effect of tube row number on effectiveness and heat exchange rate
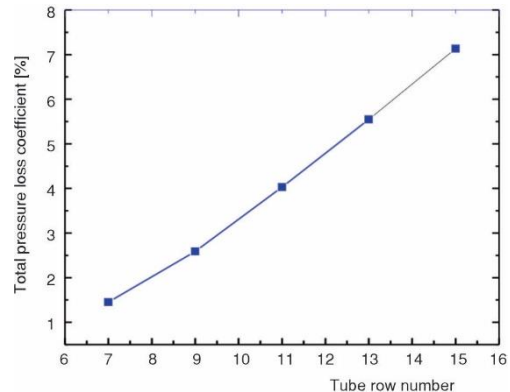

Figure 15. Effect of tube row number on total pressure loss coefficient

power only increases by 6% and effectiveness increases by 5.9%, indicating that the increase of tube row number will reduce the precooling benefit obtained by increasing the number of tube rows, which is mainly caused by the decrease of the heat transfer coefficient on the air side.

Figure 15 shows the effect of tube row number on the total pressure loss coefficient of air side. When tube row number increases from 7 to 15, the total pressure loss coefficient on the air side of the precooler increases from 1.5% to 7%. And it can be seen that the total pressure loss coefficient on the air side is approximately linearly related to tube row number.

Effect of tube transverse pitch on the heat transfer performance of air/helium precooler

The tube transverse pitch can influence the total heat transfer area of the precooler as well as the fluid velocity inside and outside the tube, which in turn influences the flow resistance and heat transfer performance of the precooler. This paper has investigated the effect of tube transverse pitch on the heat transfer of precooler under specific operating conditions with constant tube row number, total axial length of precooler, and inner and outer diameter of precooler. The compactness of the precooler corresponding to tube transverse pitch S/D is given in tab. 5.

Table 5. Relationship between tube transverse pitch S/D and compactness of precooler

Tube transverse pitch [S/D]	1.5	2	2.5	3.5
Compactness of precooler [m^2/m^3]	383.82	287.87	230.29	164.50

Figure 16 shows the variation of the average heat transfer coefficient with tube transverse pitch for the air side and helium side of the precooler. As the tube transverse pitch S/D increases from 1.5 to 3.5, the average heat transfer coefficient on the air side increases by a factor of about 4.4 and by a factor of about 2 on the helium side. It can also be seen that the heat transfer coefficient on the helium side is much larger than that on the air side. As the tube transverse pitch increases, the helium inlet velocity increases and thus the heat transfer coefficient on the helium side increases. As for the heat transfer coefficient on the air side, it might be ascribed to the reason that the reduction rate of the heat transfer area is greater than that of the heat exchange rate and the logarithmic mean temperature difference, as can be seen from figs. 17 and 18. Obviously, the average heat transfer coefficient on the air side increases according to eqs. (1) and (3).
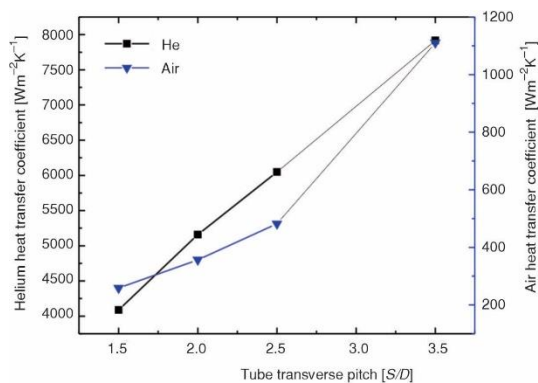

Figure 16. Effect of tube transverse pitch S/D on heat transfer coefficient of air and helium side
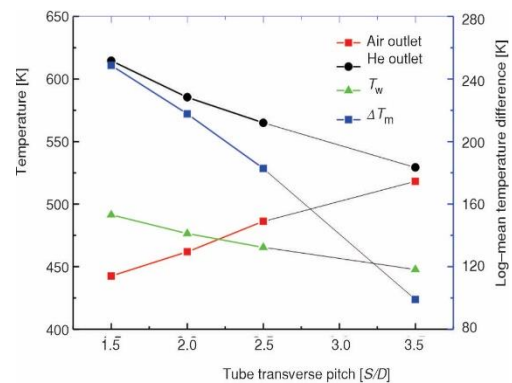

Figure 17. Effect of tube transverse pitch S/D on temperature of air, helium outlet, tube wall, and ΔT_m

Figures 17 and 18 show that effect of tube transverse pitch *S/D* on the temperature of air, helium outlet, logarithmic mean temperature ΔT_m, effectiveness and heat exchange rate of precooler. An observation can be made that the increment of tube transverse pitch *S/D* leads to the increment of the air outlet temperature, the decrement of helium outlet temperature and the average temperature of the tube wall, as well as the decrement of the heat exchange rate and effectiveness of the precooler. When the tube transverse pitch *S/D* increases from 1.5 to 3.5, the effectiveness of precooler decreases from 0.77 to 0.53, and the heat exchange rate decreases by 33 %. Although the increment of tube transverse pitch increases the heat transfer coefficient of air side and helium side, the heat transfer area and logarithmic mean temperature difference ΔT_m decreases. As a consequence, the heat exchange rate and effectiveness of the precooler decreases.
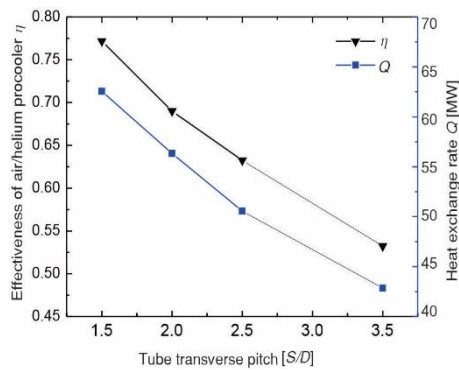

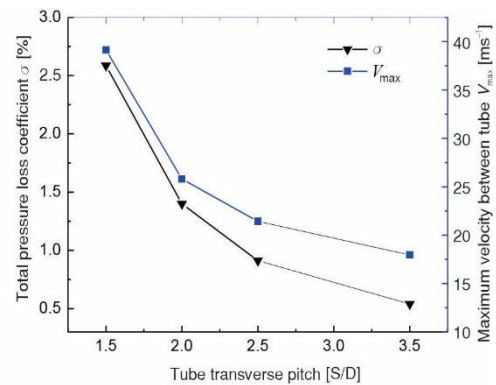**Figure 18. Effect of tube transverse pitch *S/D* on effectiveness and heat exchange rate**

Figure 19. Effect of tube transverse pitch *S/D* on total pressure loss coefficient and V_{max}

Figure 19 shows the total pressure loss coefficient, σ, on the air side of the precooler and the variation of the maximum velocity, V_{max}. between the tubes with the tube transverse pitch. It can be seen that as the tube transverse pitch increases from 1.5 to 3.5, the total pressure loss coefficient decreases from 2.6% to 0.5%. Moreover, as the tube transverse pitch increases, the decrement rate of the total pressure loss coefficient slows down and the maximum flow velocity V_{max} decreases.

Effect of helium inlet velocity on the heat transfer performance of air/helium precooler

When the structure of the precooler and the boundary conditions of the air inlet remain unchanged, the helium inlet velocity will affect the heat transfer coefficient on the helium side, thereby affecting the flow and heat transfer on the air side of the precooler. Therefore, it is necessary to investigate the effect of helium inlet velocity on the flow and heat transfer performance of the air/helium precooler.

Figure 20 shows the relationship between the average heat transfer coefficient on the air side and the helium side of the precooler with the helium inlet velocity. It can be seen that the average heat transfer coefficient on the air side and the helium side increases with the increase of the helium inlet velocity. As the helium inlet velocity increases from 5.57 m/s to 8.61 m/s, the average heat transfer coefficient on the air side increases by 30% , and the average heat transfer coefficient on the helium side increases by 40%. According to the empirical formula of heat transfer Nusselt number in the tube [30], the average heat transfer coefficient of the

924

Wei, X., *et al.*: Numerical Investigation on the Heat Transfer of …
THERMAL SCIENCE: Year 2024, Vol. 28, No. 2A, pp. 913-927

helium side is positively correlated with the helium inlet velocity. The increase of the average heat transfer coefficient on the air side is mainly due to the decrease of the logarithmic mean temperature difference, as shown in the fig. 21, and the increase of the heat exchange rate of the precooler, as shown in the fig. 22. According to eqs. (1) and (3), total heat transfer coefficient, K, increases, and thus the average heat transfer coefficient on the air side increases. Meanwhile, it can be seen that the heat transfer coefficient on the helium-side has a linear relationship with the helium inlet velocity, and the rising rate of the air-side heat transfer coefficient gradually slows down. As the helium inlet velocity increases from 5.57 m/s to 6.58 m/s, the air-side heat transfer coefficient increases by 8.9 % , while the air-side heat transfer coefficient increases only by 5.7 % with the helium inlet velocity increasing from 7.59 m/s to 8.61 m/s.
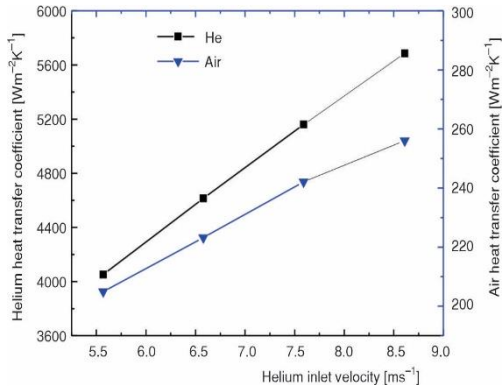

Figure 20. Effect of helium inlet velocity on heat transfer coefficient of air side and helium side
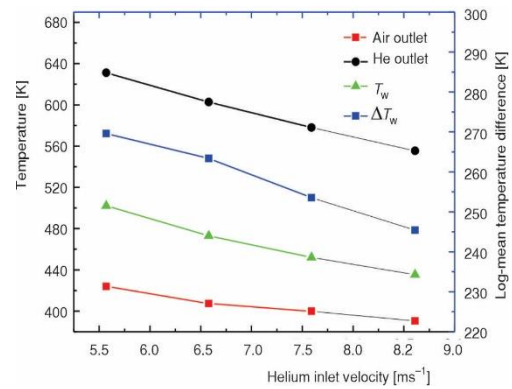

Figure 21. Effect of helium inlet velocity on temperature of air, helium outlet, tube wall, and ΔT_m

Figures 21 and 22 shows that the air outlet temperature, helium outlet temperature and average tube wall temperature decrease with the increase of helium inlet velocity, and the rate decreases gradually. However, the heat exchange rate and efficiency of the precooler increases, and the rising rate decreases with the increase of helium inlet velocity. As the helium inlet velocity increases from 5.57 m/s to 6.58 m/s, the air outlet temperature decreases by 16.5 K, and the heat exchange rate increases by 5.6%. When the helium inlet velocity increases from 7.59 m/s to 8.61 m/s, the air outlet temperature decreases by 9.3 K, and the heat exchange rate
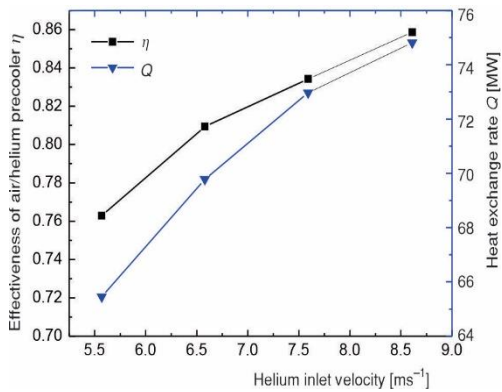

Figure 22. Effect of helium inlet velocity on effectiveness and heat exchange rate of precooler
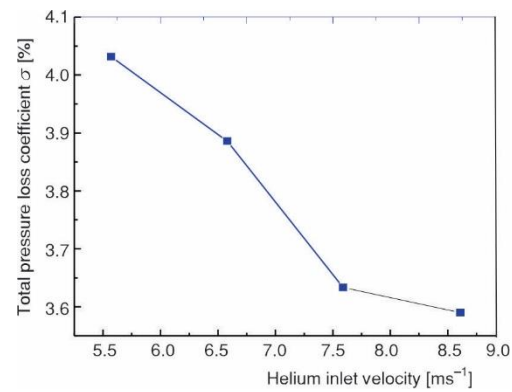

Figure 23. Effect of helium inlet velocity on total pressure loss coefficient

increases only by 2.4%. This phenomenon could be attributed to the fact that as the helium inlet velocity increases, the decrease rate of the average tube wall temperature slows down, and the increase rate of the fluid temperature gradient near the air side wall also slows down correspondently, which decelerates the increase rate of the heat exchange rate.

Figure 23 shows that the relationship between the total pressure loss coefficient on the air side with the helium inlet velocity. As the helium inlet velocity increases, the total pressure loss coefficient on the air side gradually decreases. The total pressure loss coefficient on the air side decreases from 4.03% to 3.59% with the helium inlet velocity increasing from 5.57 m/s to 8.61 m/s. This could be attributed to the fact that the increase of helium inlet velocity enhances the precooling effect of the air side, resulting in a decrease in air temperature along the path, which in turn increases air density, thus the air velocity along the flow direction slows down, making the total pressure loss on the air side decrease.

Conclusions

In this paper, we establish the minimum periodic flow and heat transfer model of the air/helium precooler. The effects of key parameters such as tube transverse pitch, tube row number, and helium inlet velocity on the heat transfer characteristics of the air/helium precooler are numerically explored. The following conclusions can be drawn:

- The increment of tube row number rn can cause pretty decrease of the heat transfer coefficient of air side, it decreases by 57% at $r_n = 15$ compared the value at $r_n = 7$. However, the heat transfer coefficient of helium side decreases only by 3.8% at rn=15 compared the value at $r_n = 7$. Thus, the increase of tube row number will reduce the precooling benefit obtained by increasing the number of tube rows. The total pressure loss coefficient on the air side of the precooler increases from 1.5% to 7% with the tube row number increasing from 7 to 15.
- When the tube transverse pitch *S/D* increases from 1.5 to 3.5, the average heat transfer coefficient on the air side increases by a factor of about 4.4 and the total pressure loss coefficient decreases from 2.6% to 0.5%. While the increase of tube transverse pitch *S/D* can reduce the heat transfer area, and thus the heat exchange rate decreases by 33%.
- The helium inlet velocity can enhance the heat transfer coefficient on the air side and heat exchange rate of precooler. As the helium inlet velocity increases from 5.57 m/s to 8.61 m/s, the average heat transfer coefficient on the air side increases by 30%, the air outlet temperature decreases by 25.8 K, and the heat exchange rate increases by 8%.
- When the tube row number increases from 7 to 15, the heat transfer area increases by 106%, the heat transfer coefficient decreases by 57%, and the heat exchange rate increases by 19.7%. When tube transverse pitch *S/D* decreases from 3.5 to 1.5, the heat transfer area increases by 134%, and heat exchange rate increases by 46%. As the helium inlet velocity increases from 5.57 m/s to 8.61 m/s, the heat exchange rate increases only by 8%. Obviously, the tube transverse pitch *S/D* has a greater impact on the heat transfer performance of the precooler than the tube row number. The helium inlet velocity has a smaller impact on the heat transfer of the precooler than tube row number and tube transverse pitch *S/D*. Therefore, on the premise of meeting the heat transfer area, the design of the precooler should give priority to the combination of smaller tube row number and smaller tube transverse pitch. In terms of the research scope of this paper, the combination of 7 rows and 1.5 *S/D* tube transverse pitch is recommended.

926

Wei, X., *et al.*: Numerical Investigation on the Heat Transfer of …
THERMAL SCIENCE: Year 2024, Vol. 28, No. 2A, pp. 913-927

Acknowledgment

Nomenclature

A – area [m^2]
c_p – specific heat capacity [Jkg^{-1}K^{-1}]
h – heat transfer coefficient [Wm^{-2}K^{-1}]
K – total heat transfer coefficient, [Wm^{-2}K^{-1}]
$\dot{m}$ – mass-flow rate [kgs^{-1}]
Q – heat exchange rate [MW]
ΔT – temperature difference [K]

Greek symbols

ε – effectiveness of precooler
σ – total pressure loss coefficient
ψ – correction factor

Acronym

SABRE – synergistic air-breathing rocket engine

References

[1] Huang, H., *et al.*, Numerical Study on Aerodynamic Heat of Hypersonic Flight, *Thermal Science, 20* (2016), 3, pp. 939-944
[2] Murthy, S. N. B , *et al.*, *Developments in High-Speed Vehicle Propulsion Systems*, Progress in Astronautics & Aeronautics, AIAA, 1996, Vol. 165, pp. 259-331
[3] Murray, J. J., *et al.*, Overview of the Development of Heat Exchangers for Use in Air-Breathing Propulsion Pre-Coolers, *Acta Astronautica, 41* (1997), 11, pp. 723-729
[4] Varvill, R., *et al.*, A Comparison of Propulsion Concepts for SSTO Reusable Launchers, *Journal of the British Interplanetary Society, 56* (2003), pp. 108-117
[5] Dong, P. C., *et al.*, Study on Multi-Cycle Coupling Mechanism of Hypersonic Precooled Combined Cycle Engine, *Applied Thermal Engineering, 131* (2018), Feb., pp. 497-506
[6] Najjar, Y. S. H., *et al.*, Enhancement of Performance of Gas Turbine Engines by Inlet Air Cooling and Cogeneration System, *Applied Thermal Engineering, 16* (1996), 2, pp. 163-173
[7] Wang, Z. G., *et al.*, Overview of the Key Technologies of Combined Cycle Engine Precooling Systems and the Advanced Applications of Micro-Channel Heat Transfer, *Aerospace Science & Technology, 39* (2014), Dec., pp. 31-39
[8] Chen, M., *et al.*, Study on Influence of Forced Vibration of Cooling Channel on Flow and Heat Transfer of Hydrocarbon Fuel at Supercritical Pressure, *Thermal Science, 26* (2022), 4B, pp. 3463-3476
[9] Sato, T., *et al.*, Development Study of a Precooled Turbojet Engine, *Acta Astronautica, 66* (2010), 7-8, pp. 1169-1176
[10] Sato, T., *et al.*, Development Study on ATREX Engine, *Acta Astronautica, 47* (2000), 2-8, pp. 799-808
[11] Varvill, R., *et al.*, The SKYLON Spaceplane, *Journal of the British Interplanetary Society, 57* (2004), pp. 22-32
[12] [12] Varvill, R., *et al.*, Heat Exchanger Development at Reaction Engines Ltd, *Acta Astronautica, 66* (2010), 9-10, pp. 1468-1474
[13] Hempsell, M., *et al.*, Progress on SKYLON and SABRE, *Proceedings*, 64th International Astronautical Congress, Beijing, China, 2013, pp. 8427-8440
[14] Davies, P.M., *et al.*, *Progress on Skylon and SABRE*, IAC-13-D2.4, 6x19609, 2015
[15] Webber, H., *et al.*, Heat Exchanger Design in Combined Cycle Engines, *Journal of the British Interplanetary Society, 62* (2009), 4, pp. 122-130
[16] Webber, H. N., *et al.*, Tunnel development for Heat Transfer Analysis in Compact Heat Exchangers, *Proceedings,* 27th Aiaa Aerodynamic Measurement Technology and Ground Testing Conference, Chicago, Ill., USA, 2013
[17] Wei, X., *et al.*, Thermodynamic Analysis of Key Parameters on the Performance of Air Breathing Pre-Cooled Engine, *Applied Thermal Engineering, 201* (2022), Part A, 117733
[18] Meng, B., *et al.*, Micromanufacturing Technologies of Compact Heat Exchangers for Hypersonic Pre-cooled Airbreathing Propulsion: A Review, *Chinese Journal of Aeronautics, 34* (2020), 2, pp. 79-103
[19] Li, S., *et al.*, Numerical Analysis of Effects of Pre-Cooler Structure Parameter on its Performance in SABRE (in Chinese), *Journal of Propulsion Technology, 43* (2022), 4, pp. 257-264

[20] Pan, X., *et al.*, Numerical Analysis of Heat Transfer and Flow Characteristics of a Precooler with a Methanol Cracking Reaction, *Case Studies in Thermal Engineering, 34*(2022), 102065
[21] Li, C.P., *et al.*, Numerical Analysis of Heat Transfer in Precooler for Hybrid Airbreathing Rocket Engines (in Chinese), *Journal of Engineering Thermophysics, 38* (2017), 4, pp. 811-816
[22] Murray, J. J., *et al.*, An Experimental Precooler for Airbreathing Rocket Engines, *Journal of the British Interplanetary Society, 54* (2001), 5/6, pp. 199-209
[23] Li, H., *et al.*, Experimental Study and Performance Analysis of High-Performance Micro-Channel Heat Exchanger for Hypersonic Precooled Aero-Engine, *Applied Thermal Engineering, 182* (2021), 116108
[24] Webber, H., *et al.*, The Sensitivity of Precooled Air-Breathing Engine Performance to Heat Exchanger Design Parameters, *Journal of the British Interplanetary Society, 60* (2007), 5, pp. 188-196
[25] Zhang J.Q., *et al.*, Thermodynamic Efficiency Analysis and Cycle Optimization of Deeply Precooled Combined Cycle Engine in the Air-Breathing Mode, *Acta Astronautica, 138* (2017), Sept., pp. 394-406
[26] Qu, Y., *et al.*, Application of Exergy Analysis in Synergistic Air-Breathing Rocket Engine (in Chinese), *Journal of Propulsion Technology, 40* (2019), 8, pp. 1693-1701
[27] Yu, X. F., *et al.*, Precooler-Design & Engine-Performance Conjugated Optimization for Fuel Direct Precooled Airbreathing Propulsion, *Energy, 170* (2019), Mar., pp. 546-556
[28] Yu, X.F., *et al.*, Thermodynamic Design and Optimization of the Multi-Branch Closed Brayton Cycle Based Precooling-Compression System for a Novel Hypersonic Aeroengine, *Energy Conversion and Management, 205* (2020), 112412
[29] Villace, V. F., *et al.*, Simulation of a Combined Cycle for High Speed Propulsion, *Proceedings,* 48th AIAA Aerospace Sciences Meeting Including the New Horizons Forum and Aerospace Exposition, Orlando, Fla., USA, 2010
[30] ***, European Space Agency, SKYLON Assessment Report, 2011
[31] Rohsenow, W. M., *Handbook of Heat Transfer*, Osborne McGraw-Hill, New York, 1973
[32] Qian, B. J., *Concise Heat Transfer Manual*, Higher Education Press, Beijing, 1983